CALCULATION OF THE EFFECT OF OXIDES AGGLOMERATION IN LIQUID STEEL CONTAINING YTTRIUM

KALISZ Dorota[1*], KUGLIN Kamil[1], GERASIN Sergiej[1], ŻAK Paweł L.[1]

[1]*AGH University of Science and Technology, Faculty of Foundry Engineering, Cracow , Poland, EU,*
dak@agh.edu.pl

Abstract

The behavior of nonmetallic inclusions in liquid steel results from such processes as fluctuation, adhesion and collisions between particles. In the metallurgical processes that take place in the ladle, the agglomeration based on turbulent collisions between oxide particles plays the most important role. Typically, the deoxidization of steel is conducted with the use of aluminum. Upon adding yttrium the process of oxides formation also refers to yttrium oxide (Y_2O_3). Both oxides have a strong grouping tendency. For this reason the collisions between particles will cover both oxides of the same and of different components. For the sake of determining the rate of turbulent collisions of aluminum oxide and yttrium oxide particles through the mixing of a hot metal bath, the Particle Grouping Method and population balance equation were used. The simulations were performed for the assumed mixing energy value for 6 exemplary size-groups. The initial number of particles, resulting from the deoxidization ability of Al and Y at given oxygen content and initial radius of the formed oxide, were assumed. The analysis of obtained results revealed that at a constant oxygen content, the increase of initial radius shortens the time of fading away of particles in all six size-groups. In the case of large inclusions, their grouping through collisions is faster; it results from the higher probability that particles of large radius will collide. Particles of a very small radius (1 μm) were observed to hardly agglomerate, and because of this were hard to remove from liquid steel.

Keywords: Agglomeration, steel casting, Y_2O_3, numerical modelling, Particle Size Grouping Method

1. INTRODUCTION

The behavior of precipitates from a liquid metallic bath stems from the cooperation of such processes as: agglomeration, adhesion and effluence, on the basis of collisions realized according to III types of collision mechanisms [1-3]. Turbulent collisions result in simultaneous and intensive removal of precipitates through flotation and increase of their size. The refining brings about solid particles (Al_2O_3, Y_2O_3, Al_2O_3 - CaO), liquid particles (60 % Al_2O_3 - CaO - SiO_2) and also solid-liquid complexes. The investigations carried out by authors proved that precipitates are not equally agglomeration-prone [2]. Liquid inclusions have typically low melting temperature, thanks to which more easily cluster forming drops, and because of the collisions, create lumps and flow out. In the case of solid particles, e.g. aluminum oxide, REM oxides, the agglomeration is quick, with clusters of inclusions as an output. This is caused by the operation of capillary forces; the intensity of attraction between particles is conditioned by the lack of wettability of these precipitates by liquid steel [3].

The agglomeration of aluminum oxide inclusions was broadly analyzed in literature [3, 5 - 7]. Yin et al. [8, 9] conducted experiments lying in the observation of capillary attraction between aluminum oxide particles in liquid steel. This created bases for stating that the capillary attraction forces act on particles of radius 3μm, in a broader range than 10 μm and it is the biggest among all analyzed inclusions. If such solids inclusions as Al_2O_3 and Y_2O_3 are present in liquid steel, their agglomeration realized through turbulent collisions may be equally intensive. It is highly probable that such complex agglomerates as Y_2O_3 - Y_2O_3, Al_2O_3 - Al_2O_3, and Al_2O_3- Y_2O_3 will be formed. However, fine Y_2O_3 precipitates play the role of a fine-dispersive phase responsible for hardening and having the function centers of crystallization and for other inclusions, e.g. nitrides and carbides [9]. From the point of view of process efficiency, their presence in the form of fine particles is

advantageous. In this case they should be evenly distributed in the steel volume, and their agglomeration is not advantageous. In this paper the Particle Size Grouping (PSG) method was used for calculating agglomeration of aluminum and yttrium oxides on the basis of the population balance equation [10]

1.1. Particle Size Grouping Method

The PSG allows to calculate the agglomeration for a small number of size groups of non-metallic inclusions, maintaining their volume balance [5-11]. The analyzed population of particles has a characteristic radius r and number in a unit of steel volume N_0. The calculating of the population balance is a huge calculation task, therefore PSG method is very helpful. It simplifies the calculation by grouping many particles into M size groups, and the population balance equation is solved only for particular size group. It has been assumed that all particles are assigned to one of size groups, which means that only particle representative for a given group is taken into account during computation, i.e. of volume from v_1 to v_M. The v_k / v_{k-1} = R ratio is constant in each group. Authors assumed R = 2, which means that the critical particle v_k is built of two particles of lower level v_{k-1}. The calculations were performed with the following equations [5, 6, 10]:

$$n_k^* = \frac{n_k}{N_0}, \tag{1}$$

$$\frac{dn_k^*}{dt^*} = \sum_{i=i_{c,k-1}}^{k-1} \xi_{i,k-1}\left(r_1^* + r_{k-1}^*\right)^3 n_i^* n_{k-1}^* + \sum_{i=1}^{i_{c,k-1}} \zeta_{i,k}\left(r_1^* + r_{k-1}^*\right)^3 n_i^* n_{k-1}^* - \sum_{i=i_{c,k}}^{M-1}\left(1+\delta_{i,k}\right)\left(r_1^* + r_{k-1}^*\right)^3 n_i^* n_{k-1}^*, \tag{2}$$

where: n_k^* - density of particles of given size n_k referred to the initial density of particles N_0, N_0 - initial density of particles (initial number of particles in a given volume), N_M - number of basic particles forming the biggest agglomeration, ξ, ζ - correction coefficients of particle density in a group, $i_{c,k-1}$ - critical size of particle, δ_{ij} - Kronecker delta (δ_{ij}=1 for i=j, δ_{ij}=0 for i≠j), t^* is dimensionless time. Parameters may be found with:

$$\xi_{i,k-1} = \left(v_i + v_{k-1}\right)/v_k, \quad \zeta_{i,k} = v_i / v_k, \quad r_k^* = r_k / r_1, \tag{3}$$

$$t^* = 1.3 \propto r_1^3 \sqrt{\varepsilon / \nu} N_0 t. \tag{4}$$

1.2. Results of simulations and discussion

The analysis was performed for a group of particles of varying initial size of 1 and 25 μm. The number of particles formed in the course of collisions is calculated on the basis of equations describing the frequency of collisions, depending on the radius and initial number of inclusions N_0. For the simplicity sake, six size groups were assumed in the analysis. The collisions were stimulated for mixing energy ε = 0.001 $m^2 \cdot s^{-3}$. The results were visualized in the form of plots showing how the particles vanish in particular size groups (n_k / N_0) in a function of dimensionless time (t*) for initial number of particles associated with the quantity of dissolved oxygen (500 and 10 ppm). Dimensionless time was determined with equation (4). Literature data referring to coefficient α considerably vary, also in reference to the results obtained with equation proposed by Higashitani [11]. Accordingly, α=1 was assumed. The number of particular nonmetallic inclusions was calculated for particular size groups depending on the amount of applied deoxidant. The obtained results are presented in **Table 1.**

Table 1 Initial number of nonmetallic inclusions N_0 in liquid metal bath for initial radius 25 μm and 50 μm (for oxygen content 10-500 ppm)

	Particle initial radius					
	25 (μm)			50 (μm)		
Oxygen content (ppm)	Al_2O_3	Y_2O_3	$(Y,Al)_2O_3$	Al_2O_3	Y_2O_3	$(Y,Al)_2O_3$
10	755443638	1673826100	2274722263	94430455	209228262	2843402823
50	3777218190	8369130499	11373611317	472152274	1046141312	1421701415
100	7554436380	16738260998	22747222634	9443044547	2092282625	28434028229
500	37772181899	83691304992	113736113168	4721522737	10461413124	14217014146

1.2.1. Calculations for Al_2O_3 particle of initial radius r = 1 and 25 (μm) and oxygen content in steel 500 ppm:

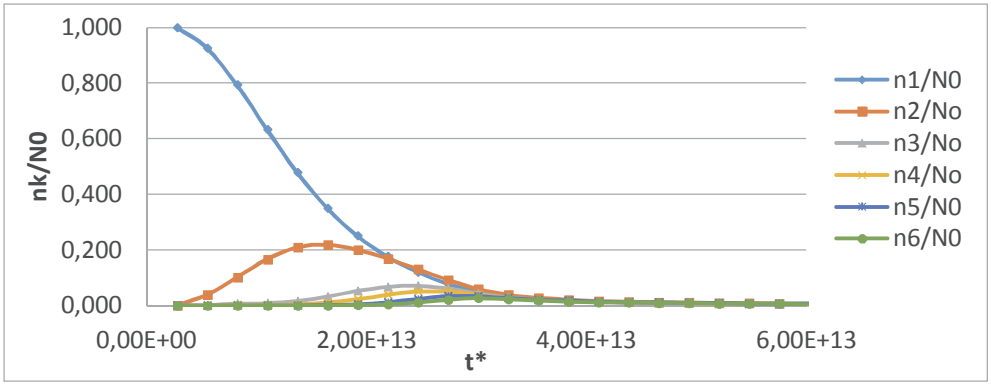

Figure 1 Results of calculations for a particle of initial radius r = 1 μm and 500 ppm [O]

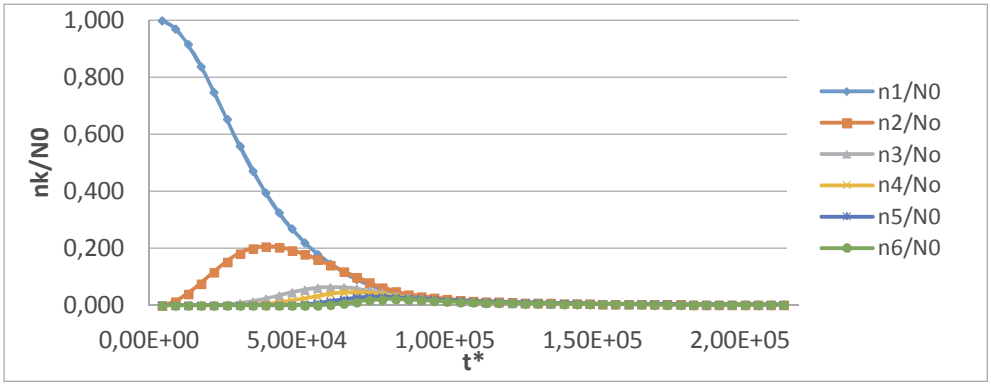

Figure 2 Results of calculations for a particle of initial radius r = 25 μm and 500 ppm [O]

Plots in **Figures 1-2** illustrate the agglomeration of Al_2O_3 particles through turbulent collision and vanishing of particles in lower groups at mixing energy ε=0.001 $m^2 \cdot s^{-3}$ for oxygen content in steel of 500 ppm. It was observed that for particles of initial size value 1 μm (**Figure 1**) agglomeration took place very slowly even when the process was considerably elongated. Their removal through collisions is difficult. The character of the plots illustrating the agglomeration of aluminum oxide inclusions and vanishing of particles from lower groups is similar to the results obtained by Higashitani et al. [11].

The same series of calculations were performed for oxygen content of 10 ppm. A considerably lower initial number of N_0 particles was obtained, which had impact on the value of calculated dimensionless time t* [7].

1.2.2. Calculations for Al_2O_3 particle of initial radius r = 1 and 25 (μm) and oxygen content in steel 10 ppm:

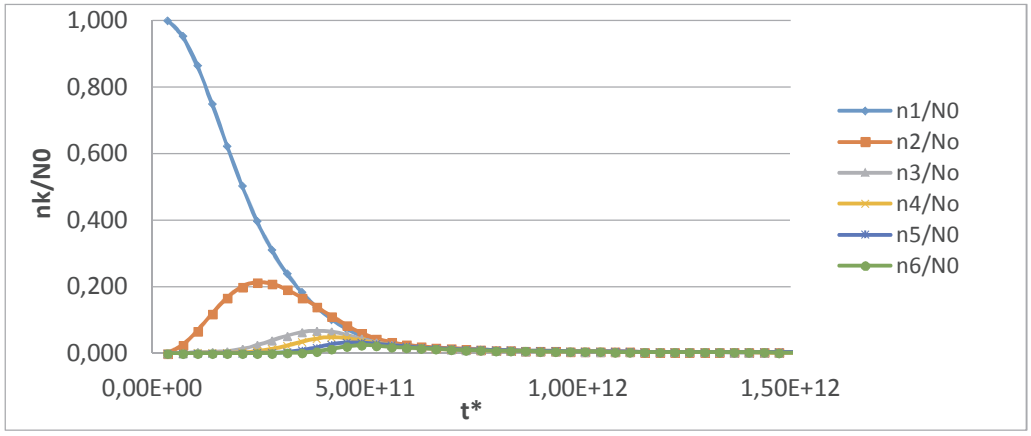

Figure 3 Results of calculations for a particle of initial radius r = 1 μm and 10 ppm [O]

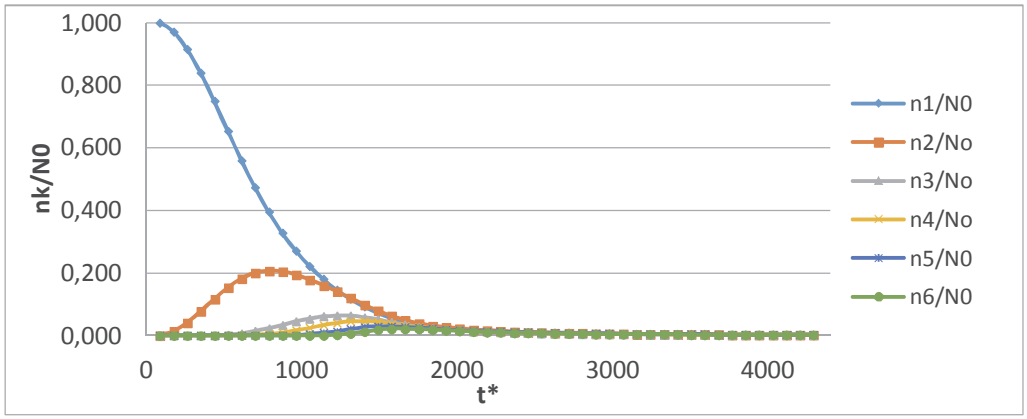

Figure 4 Results of calculations for a particle of initial radius r = 25 μm and 10 ppm [O]

The character of the plots (**Figure 3 and 4**) is similar as for the case 1.2.1, where the oxygen content equaled to 500 ppm. Analogously, the agglomeration tends to slow down for small particles (1 μm). Also in this case the agglomeration of particles of small diameter is difficult and the process has to be carried out for a long time, which in real conditions is difficult.

1.2.3. Calculations for Y_2O_3 particle of initial radius r = 1 and 25 (μm) for oxygen content in steel 500 ppm:

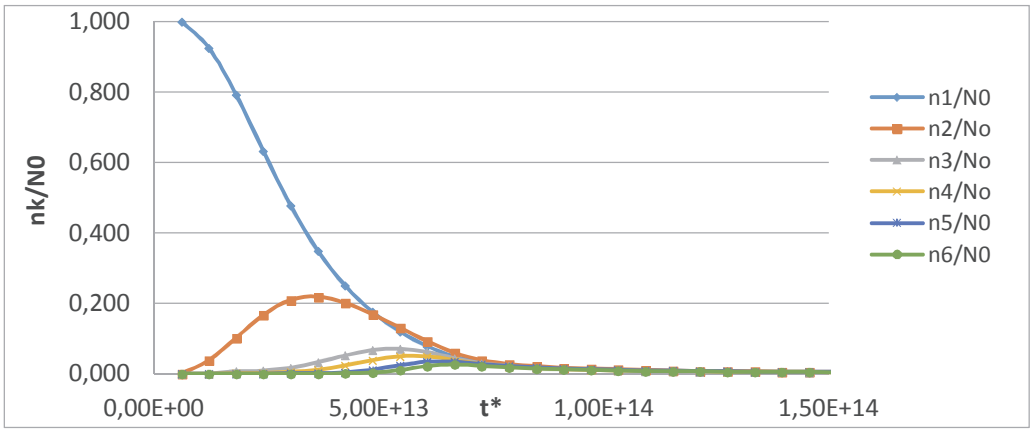

Figure 5 Results of calculations for a particle of initial radius r = 1 μm and 500 ppm [O]

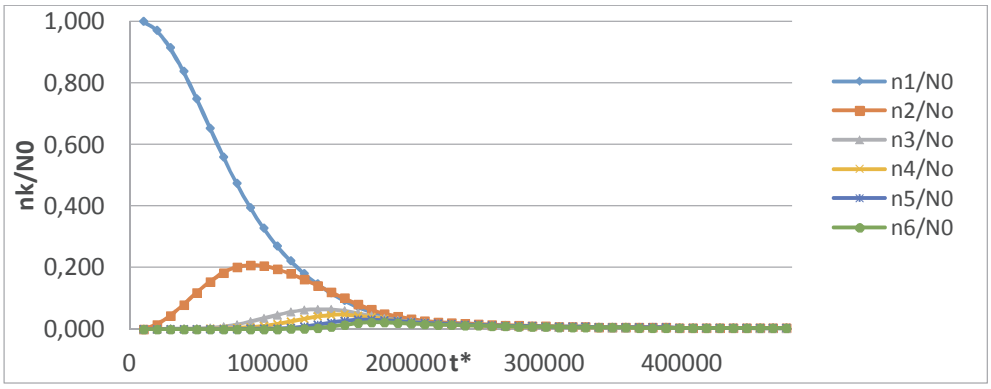

Figure 6 Results of calculations for a particle of initial radius r = 25 μm and 500 ppm [O]

As shown in **Figures 5** and **6** the Y_2O_3 inclusions, analogous to other metal oxides of rare soils, belong to compounds tending to agglomerate. The growth of yttrium oxides inclusions and reduction of particles in particular size groups was calculated for the same mixing energies and initial sizes of radius as in the case of aluminum oxide inclusions. The differences of agglomeration plots stem from the number of particles (N_0) taken into account in the calculation. The number of inclusions N_0 was determined on the basis of stoichiometry of yttrium oxide formation for oxide content 500 and 10 ppm and initial size of inclusions. The observation of the plot of Y_2O_3 particles reduction in particular size groups reveals that it has the same tendency to agglomerate as Al_2O_3. The presented examples of calculation for inclusions of initial radius 1μm prove that the increase though collision is very difficult and requires much time.

1.2.4. Calculations for Y_2O_3 particle of initial radius r = 1 and 25 (μm) and oxygen content in steel 10 ppm:

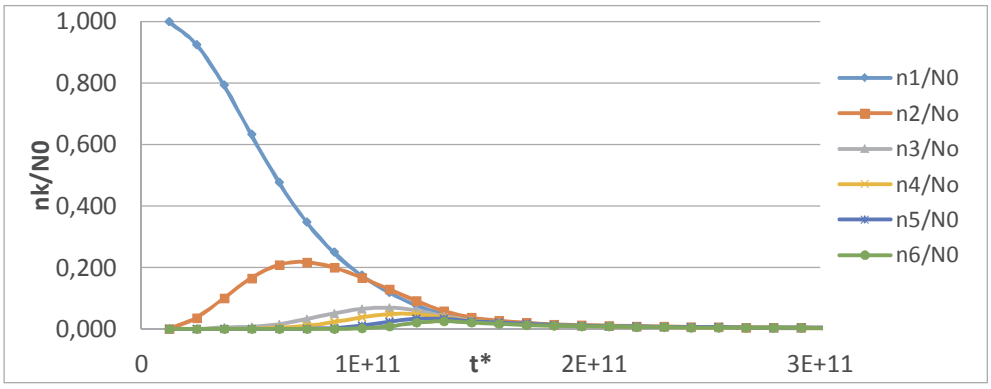

Figure 7 Results of calculations for a particle of initial radius r = 1 μm and 10 ppm [O]

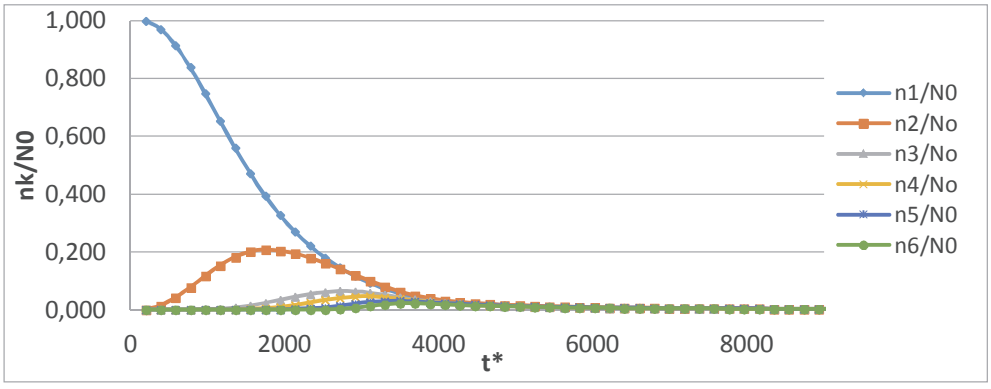

Figure 8 Results of calculations for a particle of initial radius r = 25 μm and 10 ppm [O]

1.2.5. Calculation for a particle consisting of Al_2O_3 and Y_2O_3 of initial radius r = 1 and 25 [μm] and oxygen content in steel 500 ppm:

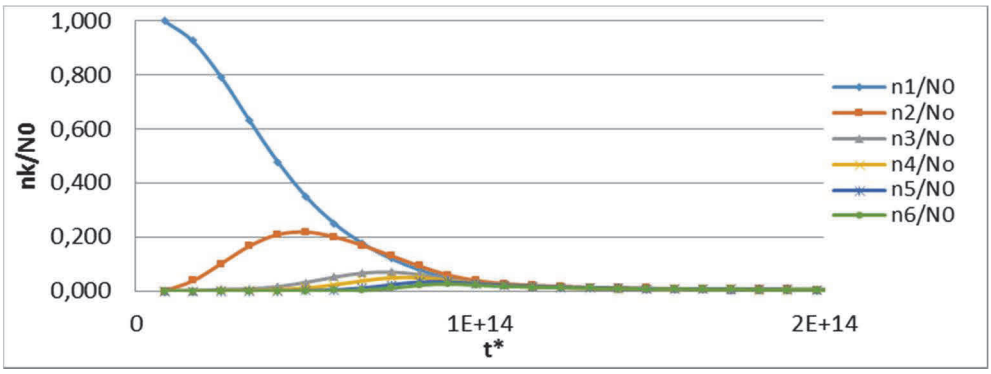

Figure 9 Results of calculations for a particle of initial radius r = 1 μm and 500 ppm [O]

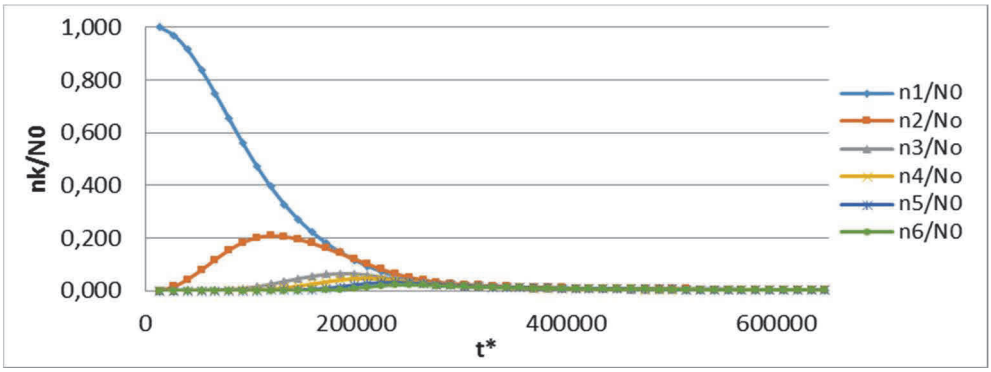

Figure 10 Results of calculations for a particle of initial radius r = 25 μm and 500 ppm [O]

The presented plots (**Figures 7 - 10**) refer to the simulation of the growth of inclusions through collisions between particles of different chemical composition. Analogous to previous cases, a time scale was assumed (dimensionless time t*). Unlike variants 1.2.1 - 1.2.4, the agglomeration was analyzed for a system of collisions taking place between Al_2O_3 and Y_2O_3 particles. In the case of inclusions of bigger initial radius, agglomeration takes place much faster, especially for particles of initial radius 1 and 25 μm. For particles of radius 1 μm the agglomeration is hindered and the course is analogous to that of pure Al_2O_3 and Y_2O_3.

1.2.6. Calculations for a particle composed of Al_2O_3 and Y_2O_3 of initial radius r = 1 and 25 (μm) and oxygen content in steel 10 ppm:

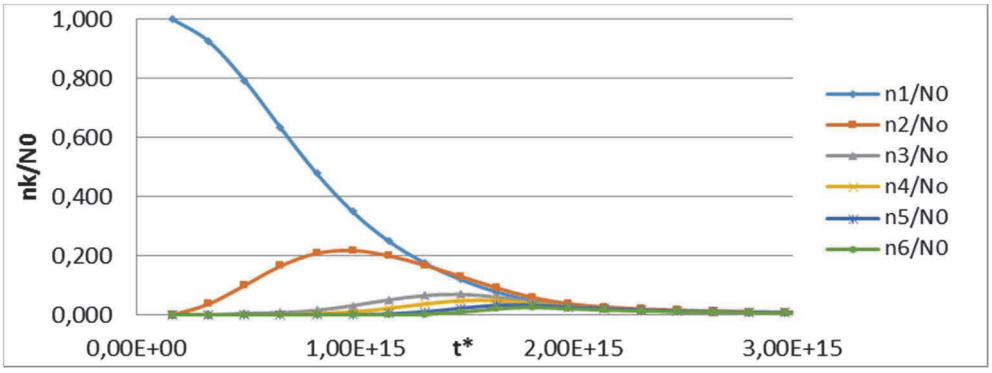

Figure 11 Results of calculations for a particle of initial radius r = 1 μm and 10 ppm [O]

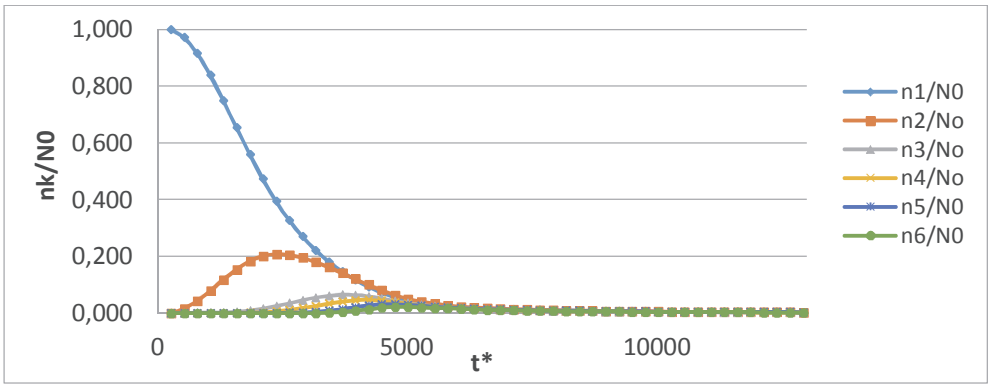

Figure 12 Results of calculations for a particle of initial radius r = 25 μm and 10 ppm [O]

The last series of calculations made for double oxides generated through the collision of inclusions obtained by the removal of oxide of initial content 10 ppm. The agglomeration plots (**Figures 11, 12**) have an analogous increase tendency and vanishing of inclusions in particular size groups as in the previous case. Similar to previous simulations, the agglomeration of inclusions of very small initial radius 1 μm is very difficult, therefore in the case of very fine precipitates diffusion should be considered. The differences in the agglomeration plots stem from the assumed initial value of N_0 for double oxides.

2. CONCLUSION

The results of simulations show the dynamics of removal of nonmetallic inclusions in a bath through turbulent collisions at a given mixing energy. Varying rates of bath mixing and initial size of particles are analyzed in the applied calculation method. The model accounts for particles removal from a given group through collisions of particles of the same group or lower group or all higher groups. This task can be handled by solving the population balance equation. The agglomeration was observed to proceed much faster for particles of bigger radius and higher mixing energies. In the case of bigger inclusions their fast agglomeration is associated with a higher probability that bigger particles will collide.

The presented plots do not show the whole mechanism of their removal, though they show the dynamics of the process. It was observed that after a given time there is always 1 % of particles representing each of the groups. Their removal is much more time-consuming because of the lower probability that they will collide. The presented results present the differences in the agglomeration of inclusions through turbulent collisions; the calculation procedure does not account for other possible phenomena which can be encountered during refining and which lead to the removal of precipitates from steel. The obtained results are analogous to the results obtained in previous experiments carried out by various scientists, i.e [11]. It is important to note, that however model helps to understand effect of oxides agglomeration it doesn't take under account all the spectrum of phenomena that took place at liquid steel.

ACKNOWLEDGEMENTS

This work was sponsored by Ministry of Science as the statute work - AGH UST - University of Science and Technology in Cracow (contract 11.11.170.318.14).

REFERENCES

[1] TOZAWA, H., KATO, Y., SORIMACHI, K., NAKANISHI, T. Agglomeration and Flotation of Alumina Clusters in Molten Steel. *ISIJ International*, 1999, vol. 39, no. 6, pp. 426-434.

[2] YIN, H., SHIBATA, H., EMI, T., SUZUKI, M., Characteristic of Agglomeration of Various Inclusion Particles on Molten Steel Surface. *ISIJ International,* 1997, vol. 37, no. 10, pp. 946-955

[3] ZHANG, J., LEE, H.G. Numerical modelling of nucleation and growth of inclusions in molten steel based on mean processing parameters. *ISIJ International*, 2004, vol. 44, no. 10, pp. 1629-1638.

[4] MIKHALOV, G.G., MAKROVETS, L.A., SMIRNOV, L.A. Thermodynamic simulation of phase equilibria of oxide systems containing rare earth metals. *Bulletin of the South Ural State University*, 2014, vol. 14, no. 4, pp. 5-10.

[5] KALISZ, D., ŻAK, P.L., KUGLIN, K. Analysis of agglomeration of Al_2O_3 particles in liquid steel. *Archives of Metallurgy and Materials*, 2016, vol. 61, no. 4, pp. 2091-2096.

[6] KALISZ, D., ŻAK, P.L. PSG Method for Simulating Agglomeration of Al_2O_3 Inclusions in Liquid Steel. *Acta Physica Polonica A*, 2016, vol. 130, no. 1, pp. 157-159.

[7] SAFFMAN, P.G., TURNER, J.S. On the Collision of Drops in Turbulent Clouds. *Journal of Fluid Mechanics,* 1956, vol. 1, no. 1, pp. 16-30.

[8] YIN, H., SHIBATA, H., EMI, T., SUZUKI, M. „In-situ" Observation of Colision, Agglomeration and Cluster Formation of Alumina Inclusion Particles on Steel Melts. *ISIJ International*, 1997, vol. 37, no. 10, pp. 936-945.

[9] SHIBATA, H., YIN, H., YOSHINAGA, S., EMI, T., SUZUKI, M. In-situ observation of engulfment and pushing of nonmetallic inclusions in steel melt by advancing melt/solid interface. *ISIJ International,* vol. 38, no. 2, pp. 149-156

[10] NAKAOKA, T., TANIGUCHI, S., MATSUMOTO, K., JOHANSEN, S.T. Particle-size-grouping method of inclusion agglomeration and its application to water model experiments. *ISIJ International*, 2001, vol. 41, no. 10, pp. 1103-1111.

[11] HIGASHITANI, K., YAMAUCHI, K., MATSUNO, Y., HOSOKAWA, G. Turbulent coagulation of particles in a viscous fluid. *Journal of Chemical Engineering of Japan*, 1983, vol. 16, no. 4, pp. 299-305.